Supplementary Information

Hydrogen storage of commercially scalable CALF-20: A study at cryogenic and near-ambient temperatures

Ashley L. Sutton, *[a] M. Munir Sadiq, [a] James I Mardel [a] and Matthew R. Hill [a,b]

[a.] *Manufacturing, CSIRO, Private Bag 33, Clayton South MDC, Victoria, 3169, Australia*
[b.] *Department of Chemical and Biological Engineering, Monash University, Clayton, Victoria, 3168, Australia*

CONTENTS

1. Experimental & Theoretical methods

Synthesis of CALF-20:

CALF-20 was synthesised using a literature method.[1]

Powder X-ray diffraction

The sample was placed on a silicon zero-background plate within a steel holder. X-ray diffraction data were collected using a Bruker D8 Advance A25 X-ray Diffractometer, using CuKα radiation equipped with a Lynx Eye XE-T detector.

Gas sorption measurements

Measurements were conducted using a volumetric sorption analysers.

1) Micrometrics, ASAP 2420 for N_2 77 K isotherm.

2) Micrometrics, 3Flex for H_2 77 K, 87 K and 298 K in the range of 0 to 1 bar.

3) SETARAM, PCT Pro for high pressure (up to 80 bar) H_2 measurements at near-ambient temperatures

In each case, prior to measurement the sample was degassed under dynamic vacuum at 150°C for 12 hours to remove any adsorbed species. Approximately 0.10 – 0.15 g of CALF-20 was subjected to gas sorption experiments.

Monte Carlo isotherms

Monte Carlo calculations were performed within the Monte Carlo and Molecular Dynamic (MCMD) Simulation software.[2] The simulation environment was setup to model hydrogen sorption in CALF-20, using the structure in the Cambridge Structural Database (CSD), deposition number 2084733. A supercell composed of 2x2x2 unit cells was utilized for all calculations. The Universal Force Field (UFF) was utilised for the Leonard-Jones potentials of the framework.[3] The hydrogen potential known as the Belof/Stern/Space model (BSS) was used for all calculations.[4] Partial atomic charges were not utilized in this study. To this end, the simulation box was populated with MOF crystal structure and hydrogen molecules were introduced at controlled fugacities to mimic experimental conditions. Monte Carlo steps totalling 1 million were performed to ensure thorough sampling of the system. Calculations were systematically varied to cover the range between -50 C to + 50 C, and 0 bar and 100 bar, reflecting realistic near-ambient temperature hydrogen storage scenarios. All calculations were scaled with single point factor to align with experimental isotherms. To reduce statistical

noise, which can become pronounced at high adsorbate loadings, we averaged the results from five independent Monte Carlo simulations for the 77 K isotherm.

Density Functional Theory (DFT) calculations

DFT calculations were conducted utilizing Quantum Espresso,[5,6] with the initial structure for CALF-20 obtained from the Cambridge Structural Database (CSD), deposition number 2084733. An energy cutoff of 1360 eV was selected based on preliminary tests, which ensured energy values accurate to at least 1.0 meV/atom. The Perdew-Burke-Ernzerhof (PBE) functional served as the basis for all calculations.[7] To account for long-range van der Waals interactions, the DFT-D3 empirical correction method was employed.[8,9] A single gamma centred k-point was used. The atomic positions and cell parameters of the CALF-20 framework were relaxed. In a subsequent calculation a hydrogen molecule was relaxed within the framework whilst cell parameters and atomic positions of the CALF-20 remained fixed. This allowed for the determination of the hydrogen binding site in addition to binding enthalpy. Binding enthalpies were calculated as $E_{bind} = E_{MOF\text{-}H2} - (E_{MOF} + E_{H2})$.

Two-dimensional heatmaps were generated to visualize the energy associated with the H_2 molecule position within the framework. To generate the 2D heatmaps a series of self-consistent field (SCF) calculations were systematically carried out wherein the H_2 molecule was moved at 0.1 fractional coordinates along all three axes. The outcomes of these calculations were illustrated through 2D heatmaps, created with group-own code.

2. Powder X-ray diffraction pattern

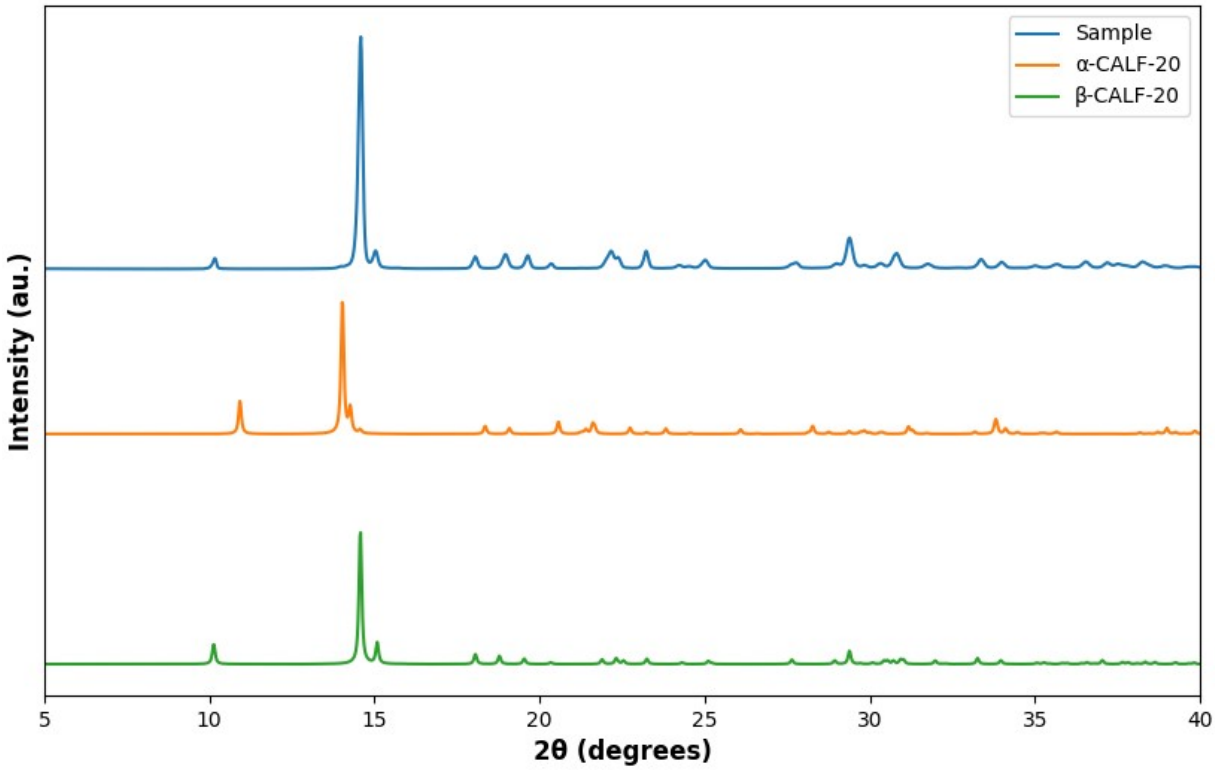

Figure S1. Powder X-diffraction pattern of the synthesised CALF-20 (blue), compared to α-CALF-20 (orange) and β-CALF-20 (green).

3. N_2 77 K Isotherm

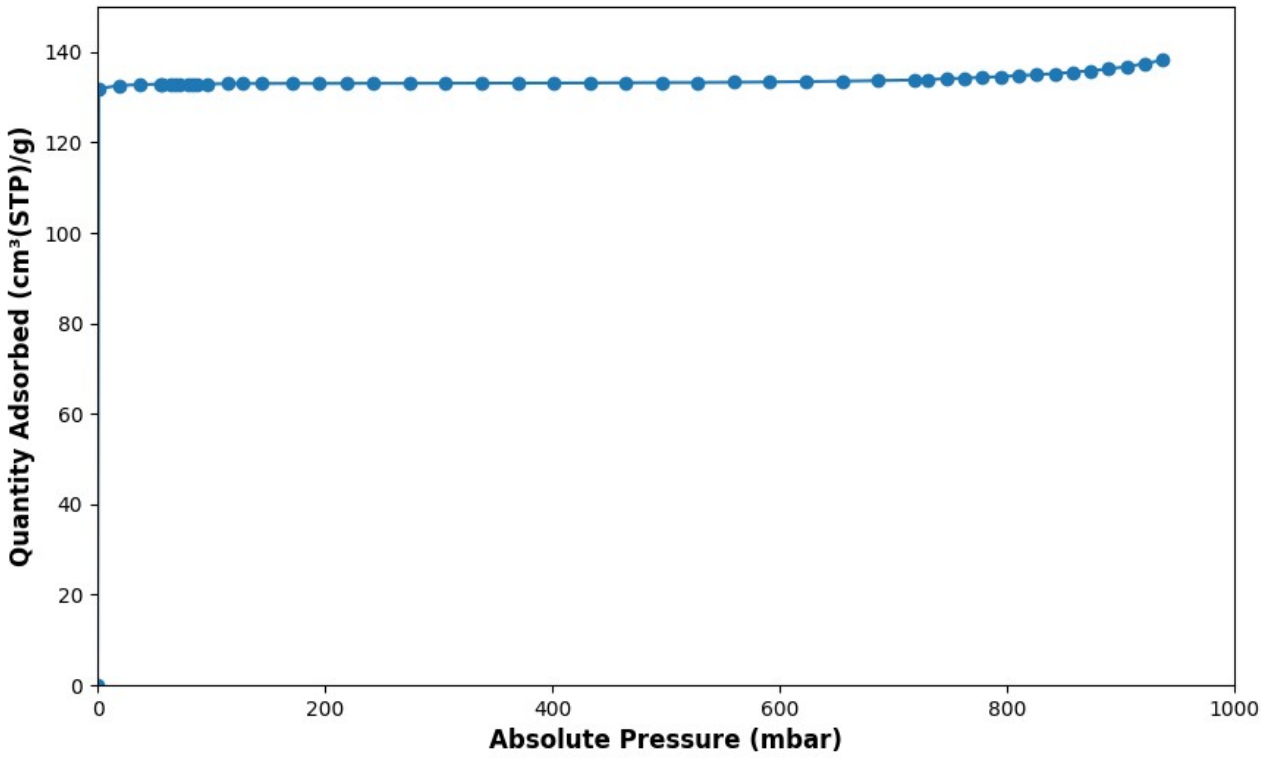

Figure S2. 77 K N_2 isotherm of CALF-20.

4. Monte Carlo isotherms

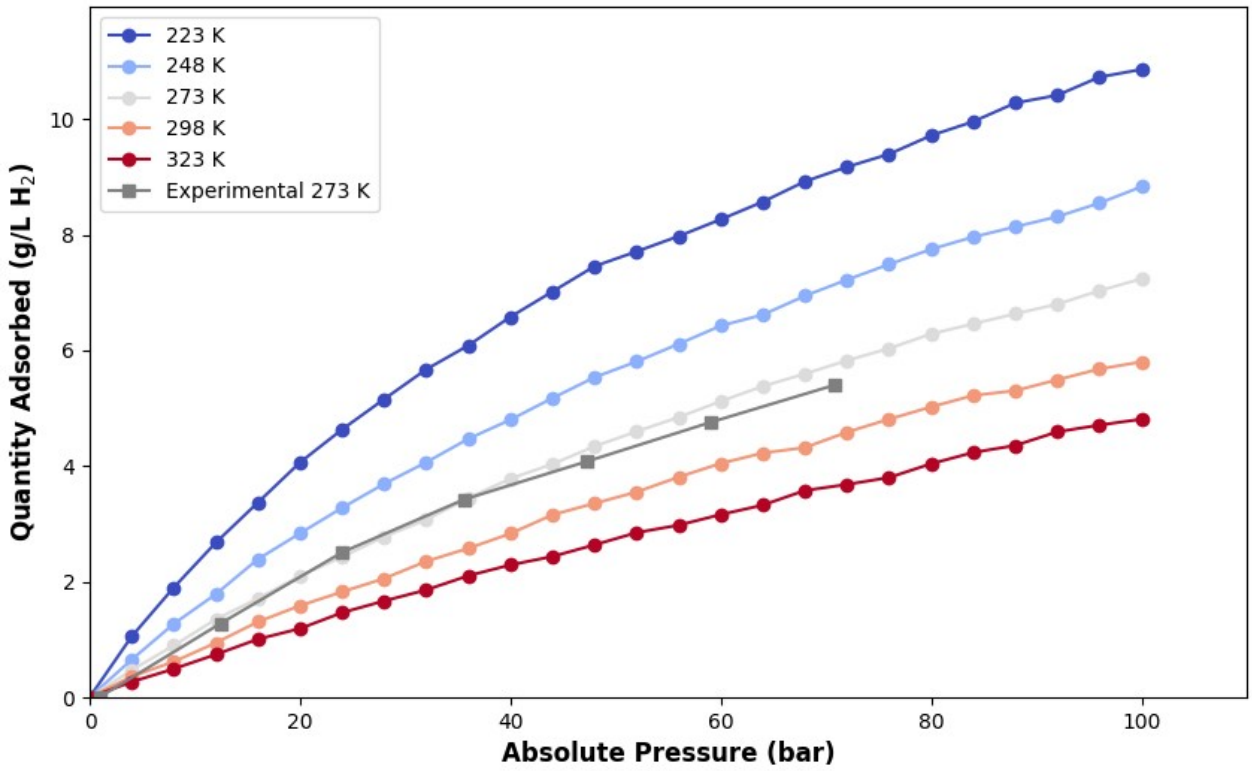

Figure S3. Simulated isotherms with Monte Carlo between 0 and 100 bar for CALF-20 at near-ambient temperatures.

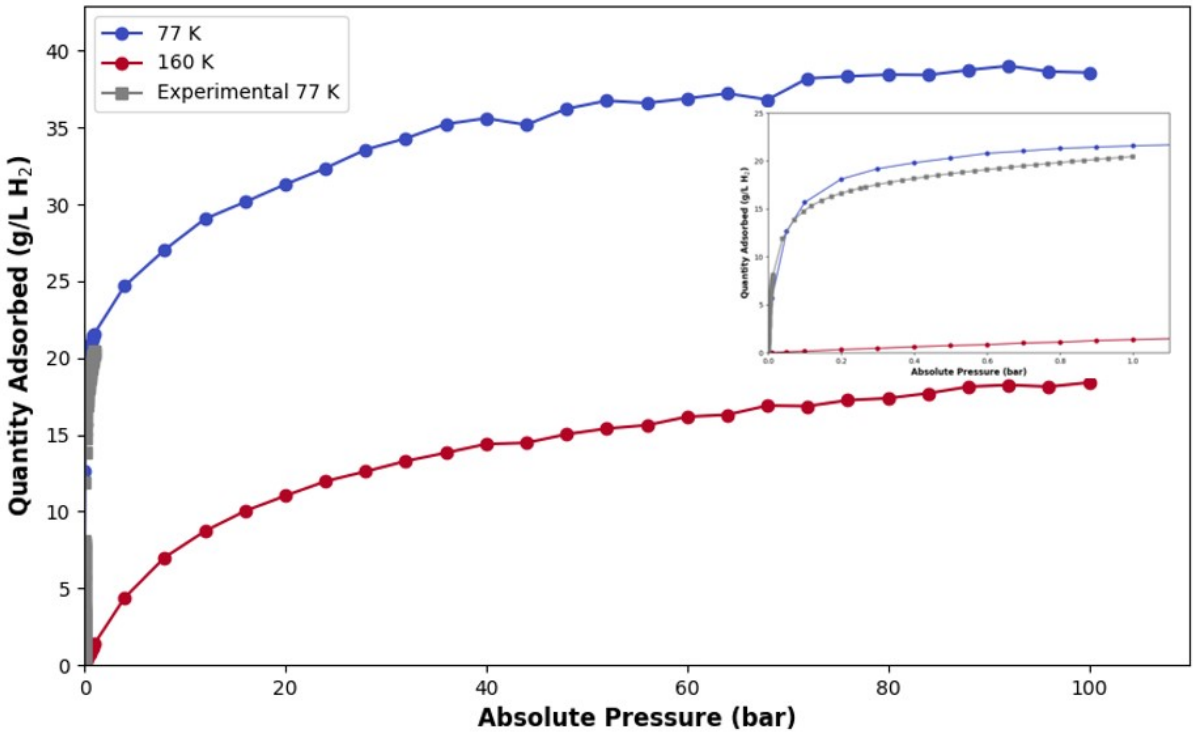

Figure S4. Simulated isotherms with Monte Carlo between 0 and 100 bar for CALF-20 at cryogenic temperatures.

5. Cost analysis & price performance ratio

A cost analysis was conducted to allow the calculation of price performance ratio. The synthesis of several metal-organic frameworks (MOFs) at the kilogram scale, specifically focusing on CALF-20, NU-2100, Ni_2(m-dobdc), and Mn-BTT was analysed in terms of cost.

Table S1. Breakdown of cost for manufacturing 1kg of CALF-20.

MOF	**Reactants**		
CALF-20	Zinc oxalate	1,2,4-triazole	Methanol (litres)
Synthesis ratio, weight	1	0.758	34
Cost USD$ / kg or L	2.5	8.8	0.62
Supplier	Alibaba	Alibaba	Chemanalyst
Yield	1 Zinc oxalate : 1.1 CALF-20		
Component cost USD$	2.3	6.0	20.9
Total cost, USD$/ kg		**29**	

Table S2. Breakdown of cost for manufacturing 1kg of NU-2100.

MOF	**Reactants**			
NU-2100	BTT	$ZnCl_2$	$CuCl_2$	DMF (Litres)
Synthesis ratio, weight	0.267	1	0.667	38
Cost USD$ / kg or L	40 Estimate	8.0 Alibaba	5.5 Alibaba	1.0 Shandong Bairui Fine Chemicals
Supplier				
Yield		4.5 $ZnCl_2$: 1 NU-2100		
Component cost USD$	48	36	17	38
Total cost, USD$ / kg		**139**		

Table S3. Breakdown of cost for manufacturing 1kg of Ni_2(m-dobdc).

MOF	**Reactants**			
Ni_2(m-dobdc)	$NiCl_2$	m-dobdc	DMF (litres)	Methanol (litres)
Synthesis ratio	1	0.612	20	12
Cost USD$ / kg or L	6.0	22	1.0	0.62

Supplier	Alibaba	*Energy Fuels* 2017, 31, 2, 2024–2032	Shandong Bairui Fine Chemicals	Chemanalyst
Yield		1.9 NiCl2 : 1 Ni_2(m-dobdc)		
Component cost USD$	11.4	25.5	20.0	7.4
Total cost, USD$ / kg		**64**		

Table S4. Breakdown of cost for manufacturing 1kg of Mn-BTT.

MOF	**Reactants**			
Mn-BTT	$MnCl_2.4H_2O$	H_3BTT	DMF (litres)	Methanol (litres)
Synthesis ratio	1	0.225	77	77
Cost USD$ / kg or L	1.96	40	1	0.616
Supplier	Alibaba	Estimate	Shandong Bairui Fine Chemicals	Chemanalyst
Yield		3.1 MnCl2 : 1 Mn-BTT		
Component cost USD$	6.06	27.9	12	7
Total cost, USD$ / kg		**53**		

Table 5. Price performance ratio of CALF-20, NU-2100, Ni_2 (m-dobdc), Mn-BTT for average binding energy between 0.01 and 3.0 mmol/g for H_2.

MOF	**Initial binding enthalpy (kJ/mol)**	**Average binding enthalpy (kJ/mol)**	**Cost per kg (USD$ / kg)**	**Price performance ratio (x 10)**
CALF-20	-7.9	-8.1	29	2.77
NU-2100	-32	-9.2	139	0.66
Ni_2(m-dobdc)	-12.3	-10.7	64	1.66
Mn-BTT	-10.1	-6.8	53	1.27

6. References

1 T. T. T. Nguyen, J. Bin Lin, G. K. H. Shimizu and A. Rajendran, *Chemical Engineering Journal*, 2022, **442**, 136263.

2 D. M. Franz, J. L. Belof, K. McLaughlin, C. R. Cioce, B. Tudor, A. Hogan, L. Laratelli, M. Mulcair, M. Mostrom, A. Navas, A. C. Stern, K. A. Forrest, T. Pham and B. Space, *Adv Theory Simul*, 2019, **2**, 1900113.

3 A. K. Rappe, C. J. Casewit, K. S. Colwell, W. A. Goddard III and W. M. Skiff, *J. Am. Chem. Soc*, 1992, **114**, 10024–10035.

4 J. L. Belof, A. C. Stern and B. Space, *J Chem Theory Comput*, 2008, **4**, 1332–1337.

5 P. Giannozzi, O. Andreussi, T. Brumme, O. Bunau, M. Buongiorno Nardelli, M. Calandra, R. Car, C. Cavazzoni, D. Ceresoli, M. Cococcioni, N. Colonna, I. Carnimeo, A. Dal Corso, S. De Gironcoli, P. Delugas, R. A. Distasio, A. Ferretti, A. Floris, G. Fratesi, G. Fugallo, R. Gebauer, U. Gerstmann, F. Giustino, T. Gorni, J. Jia, M. Kawamura, H. Y. Ko, A. Kokalj, E. Küçükbenli, M. Lazzeri, M. Marsili, N. Marzari, F. Mauri, N. L. Nguyen, H. V. Nguyen, A. Otero-De-La-Roza, L. Paulatto, S. Poncé, D. Rocca, R. Sabatini, B. Santra, M. Schlipf, A. P. Seitsonen, A. Smogunov, I. Timrov, T. Thonhauser, P. Umari, N. Vast, X. Wu and S. Baroni, *Journal of Physics Condensed Matter*, 2017, **29**, 465901.

6 P. Giannozzi, S. Baroni, N. Bonini, M. Calandra, R. Car, C. Cavazzoni, D. Ceresoli, G. L. Chiarotti, M. Cococcioni, I. Dabo, A. Dal Corso, S. De Gironcoli, S. Fabris, G. Fratesi, R. Gebauer, U. Gerstmann, C. Gougoussis, A. Kokalj, M. Lazzeri, L. Martin-Samos, N. Marzari, F. Mauri, R. Mazzarello, S. Paolini, A. Pasquarello, L. Paulatto, C. Sbraccia, S. Scandolo, G. Sclauzero, A. P. Seitsonen, A. Smogunov, P. Umari and R. M. Wentzcovitch, *Journal of Physics Condensed Matter*, 2009, **21**, 395502.

7 J. P. Perdew, K. Burke and M. Ernzerhof, *Phys Rev Lett*, 1996, **77**, 3865–3868.

8 S. Grimme, S. Ehrlich and L. Goerigk, *J Comput Chem*, 2011, **32**, 1456–1465.

9 S. Grimme, J. Antony, S. Ehrlich and H. Krieg, *Journal of Chemical Physics*, 2010, **132**, 154104.